CHAPTER 71

THE DYNAMICS OF OSCILLATING SHEETFLOW

by ir. W.T. Bakker [1] and ir. W.G.M. van Kesteren [2].

1.ABSTRACT.
Two mathematical models for the simulation of the dynamics of sheetflow are presented, an analytical and a numerical one.
In the analytical model the theory of Bagnold (1954) is implemented: a constant ratio between shear stress and normal stresses is assumed.
In the numerical model the motion of each layer of grains is considered separately; each layer exists of a rigid rectangular structure of spherical grains. Grain- grain interaction between the successive layers occurs in two ways: on one hand viscous interaction forces, comparable with squeezing forces in lubrication problems and on the other hand direct contact with elastic response when the distance between the grains becomes less than .01 of the grain diameter. When the relative motion of adjacent layers results into compression or dilatation, a resistant force analogous to the Darcy law is assumed.The numerical model has been combined with the turbulent-boundary layer model of Bakker and v. Kesteren (1984).
Results of computations are compared with measurements of Bagnold (1954) and Horikawa et al (1982).
The analytical model predicted the concentration in the sheet flow layer and the intrusion depth rather well, where the numerical model gave reasonable results with respect to the velocity pattern above the sheetflow layer.
It is concluded, that up to now the more sophisticated assumptions of the numerical model do not lead as yet to higher accuracy with respect to the intrusion depth of the sheet flow, probably because the separation between sheet flow and the turbulent boundary layer above has been assumed too smooth.

2. INTRODUCTION.

In this paper two mathematical models for the simulation of the dynamics of sheetflow are presented, an analytical and a numerical one.
Apart from the approach, also the physical schematization of both models is quite different.
In both models it is taken into account, that at high velocities a thicker layer is moving than during the time lapses with lower velocities.
In the analytical model (Ch. 3) the theory of Bagnold (1954) is implemented: a constant ratio between shear stress and normal stresses is assumed.
In the numerical model (ch.4) the motion of each layer of grains is

[1]Scientific Coordinator Coastal Research, Tidal Waters Department Rijkswaterstaat; Principal Scientific Officer Delft University of Technology
[2]Engineer Delft Hydraulics Laboratory

considered separately; each layer exists of a rigid rectangular structure of spherical grains.
Grain- grain interaction between the successive layers occurs in two ways: on one hand viscous interaction forces, comparable with squeezing forces in lubrication problems and on the other hand direct contact with elastic response when the distance between the grains becomes less than .01 times the grain diameter. When the relative motion of adjacent layers results into compression or dilatation, a resistant force analogous to the Darcy law is assumed.
Results of computations are compared with measurements of Bagnold (1954) and Horikawa et al (1982) (ch.4.2). This leads to the conclusions, given in ch 5.

3. ANALYTICAL COMPUTATIONS.

3.1 Assumptions

For the analytical computations the theory of Bagnold (1954),(1956), concerning bed load in a uniform flow, is used. According to this theory it is assumed that a dispersive pressure P proportional to the grain shearstress T is exerted on the grains. In the viscous region Bagnold finds:

$$T=.75\ P \tag{1a}$$

where T is related to the velocity gradient $\frac{du}{dz}$ in the following way:

$$T = 2.2\ \lambda^{3/2}\rho_w\nu\ \frac{du}{dz} \tag{1b}$$

in which ρ_w=spec. density water, ν=kin. viscosity, u=horizontal velocity, z=vertical coördinate (pos. upwards); λ is the linear concentration as defined by Bagnold (1954):

$$\lambda = [(c_0/c)^{1/3} - 1]^{-1} \tag{1c}$$

Here c is the concentration, having a maximum c_0.This maximum belonging to the maximum packing density, equals .74, assuming a tetrahedral rectangular piling as depicted in fig 1 and 8.
The validity of the viscous region for the sheetflowphenomena can be estimated with the Bagnold-number:

$$N = \frac{\rho_s\sqrt{\lambda}\ D^2}{\rho_w\nu}\ \frac{du}{dz} < 40 \tag{2}$$

in which D = grain diameter and ρ_s= spec. density sand.
Substitution of ρ_s/ρ_w=2.65, λ=10, D=.2 mm, $\nu=10^{-6}m^2/s$ and $\frac{du}{dz}$ =100 s^{-1} yields: N = 34 .
In a first order harmonic solution the shear stress T is given by:

$$T = \hat{T}\ \sin\omega t \tag{3}$$

Starting with the assumption in eq.(1), eq.(3) yields for the dispersive pressure:

$$P = \hat{P}\ |\sin\omega t| \tag{4}$$

where ω is the angular frequency of the motion and t is the time; the superscript "^" denotes a top value. Furthermore it is assumed, that

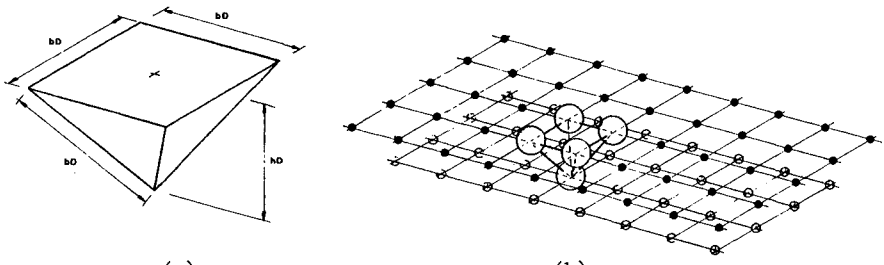

(a) (b)

Fig.1 Configuration of moving grain layers.

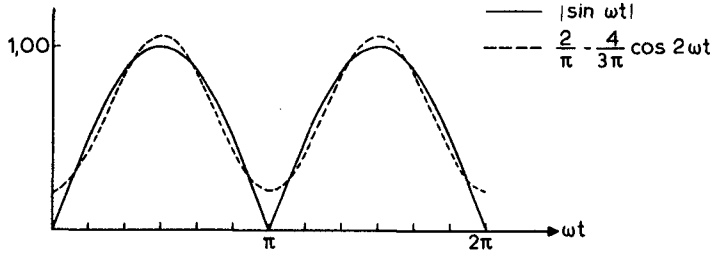

Fig.2 Mean and second harmonic of vertical pressure gradient (p).

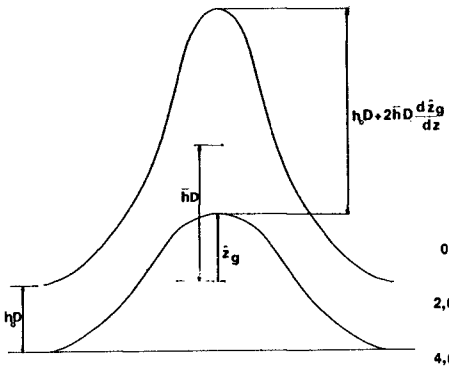

Fig.3 Vertical motion of two adjacent grain layers.

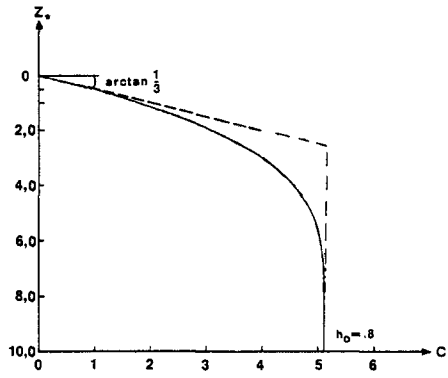

Fig.4 Mean concentration profile in the sheetflow (anal.sol.).

at the moments of rest during the changing of the direction of the oscillation the concentration is constant over the height of the sheet flow layer. The mixture of sand and water in this layer is assumed to be uniformly distributed in horizontal direction and is supposed to oscillate by means of the horizontal pressure gradient and the drag force acting on the grains.

3.2. Analysis.
Where D is the grain diameter, let hD be the mutual vertical distance between the center of two adjacent layers of grains of the sheet flow, when the grains attain their time-averaged vertical position (fig.1a). Then the vertical force p, acting on a layer of grains equals:

$$p = - hD \frac{\partial P}{\partial z} |\sin \omega t| \tag{5}$$

This vertical force can be approximated by its time-average p_0 and its second harmonic, having an amplitude $\hat{p}_2$ (fig 2):

$$p_0 = \frac{2}{\pi} hD \frac{\partial \hat{P}}{\partial z} ; \qquad \hat{p}_2 = \frac{4}{3\pi} hD \frac{\partial \hat{P}}{\partial z} \tag{6}$$

Averaged over the wave period, p_0 should balance the weight of one layer of grains.
Furthermore, the second harmonic is counteracted by the vertical drag force $a.\dot{z}_g$, where $\dot{z}_g$ denotes the time-derivative of the vertical position z_g of a grain and "a" denotes a drag coefficient:

$$a = \frac{3\pi \rho_w \nu}{b^2 D (1-c)^3} \tag{7}$$

The drag coefficient is according to Stokes, only hindered settling has been taken into account by means of $(1-c)^3$, where c is the concentration. In (7) bD denotes the horizontal distance between the grains. From the dynamic equation for the second harmonic, $\hat{z}_g$ can be expressed in p_2 and a:

$$\hat{z}_g = \hat{p}_2/(2\omega a) \tag{8}$$

Let the grains in closest packing have a distance h_0D to each other: $h_0 \cong .8$. This is reached everywhere at the moment of turning of the direction of the orbital velocity. However, $^1/_4$of a wave period later, the porosity is different everywhere, because of the vertical gradient of the vertical motion: the upper grain dances more vigorously than the lower one (fig 3). Therefore, the time-averaged distance between the grains equals:

$$\bar{h}D = h_0D + \bar{h}D \frac{\partial}{\partial z} (\hat{z}_g) \tag{9}$$

Thus the time-mean vertical spacing between the grains can be expressed in the variation of the vertical pressure p_2. However, this value $\hat{p}_2$ equals $(2/3)p_0$, according to (6), p_0 being equal to the weight of a grain layer. Thus from (8) it shows, that z_g only varies in vertical sense because the concentration varies in vertical sense. One thus understands, that (9) is essentially a differential equation in the concentration, as also h can be expressed in the concentration:

$$h = (1/\sqrt{2})(c_0/c)^{1/3} \tag{10}$$

After some elaboration (cf. Bakker & v.Kesteren (1982)), one finds the dimensionless equation:

$$\frac{\partial c}{\partial z^*} = \{h_0\sqrt{2}.(c/c_0)^{1/3} - 1\}/\{3(1 - c^2)\} \tag{11}$$

$$z^* = z/Z; \quad Z = \frac{1}{54}\,\frac{\rho_s - \rho_w}{\rho_w}\,\frac{g\,D^2}{\omega\,\nu} \tag{12}$$

Eq (11) has been solved, using Simpson's integration method, thus giving c as function of z (fig 4)
A first approximation for the time dependent concentration can be found from the mean concentrationprofile resulting from eq.(11).
Neglecting phase shifts a first order time dependent distance between the grains is given by ($\bar{h}$ denoting the mean value of h):

$$h(t)D = \bar{h}D + (\bar{h}D - h_0D)\sin(2\omega t) \tag{13}$$

Substituting eq.(10) into (13) gives for the timedependent concentration (fig 4) (c_ℓ denoting the limiting value of the concentration in the sheetflow):

$$\frac{c(t)}{c_\ell} = [(\frac{\bar{c}}{c_\ell})^{-1/3} - \{(\frac{\bar{c}}{c_\ell})^{-1/3} - 1\}\sin 2\omega t]^{-3} \tag{14}$$

$$\text{where } c_\ell = \frac{c_0}{(h_0\sqrt{2})^3} \tag{15}$$

Also a first approximation for the intrusiondepth of the sheetflow layer as function of time can be made. Schematizing more rigorously than before, the concentration in the moving sheet layer can be assumed as constant.
As the pressure increases linearly with the depth the grain shear stress also increases linearly and thus (for viscous flow) a parabolic velocity distribution is found (fig 5):

$$u = \hat{U}\,(1 - \frac{z^2}{H^2})\cos\omega t \text{ when } z \leq H \tag{16}$$

$$u = 0 \qquad \text{when } z > H$$

where $\hat{U}$ is the maximum velocity at the top of the sheetflow layer and equals the maximum velocity in the wave boundary layer; H is the time-dependent intrusion depth or thickness of sheetflow layer given by:

$$H = \hat{H}\sqrt{|\cos\omega t|} \tag{17}$$

where $\hat{H}$ is the maximum intrusion depth.
From eq. (1b), (1c) and (16) results for the shear stress:

$$T = 4.4\,\rho_w\nu\,[(\frac{c}{c_0})^{1/3} - 1]^{-3/2}\,\frac{\hat{U}\,.z}{H^2} \tag{18}$$

This is accompanied by a dispersive pressure gradient given by:

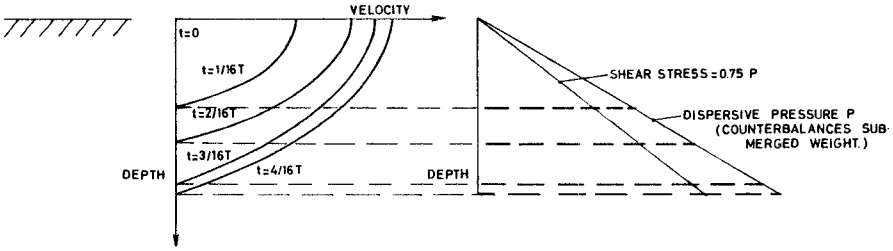

Fig.5 Assumed velocity and stress distribution in the sheetflow (anal.)

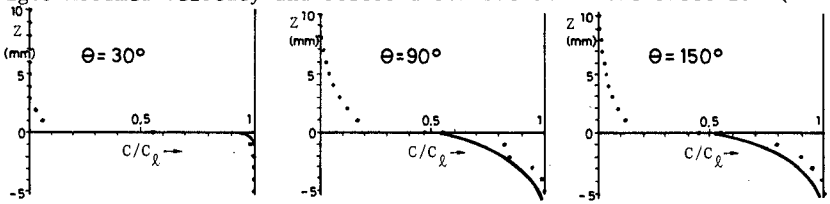

• measurements from Horikawa (1982)
—— analytical theory

Fig.6 Concentration profiles in the sheetflow (anal. comp.).

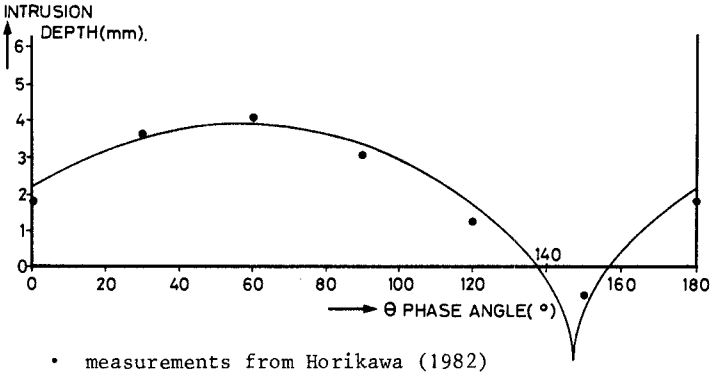

• measurements from Horikawa (1982)
—— analytical theory

Fig.7 Intrusion depth as function of time (anal. comp.).

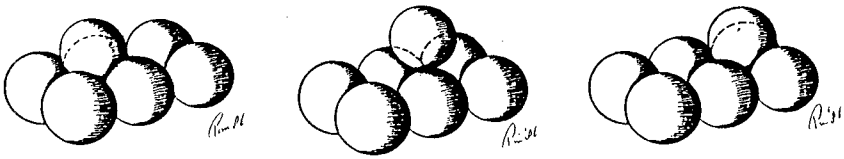

Fig.8 Relative grain motion in two adjacent layers.

$$\frac{\partial P}{\partial z} = 4.4\ \rho_w \nu\ [(\frac{c}{c_0})^{1/3} - 1]^{-3/2}\ \frac{\hat{U}}{H^2}\ \text{cotan}\ \alpha \tag{19}$$

where α is the angle of internal friction. ($\tan\alpha = .75$; eq (1a)) Because this pressure gradient must counterbalance the gravity forces on the (submerged) grains an expression for H can be found:

$$\hat{H} = \sqrt{4.4\ \frac{\rho_w}{\rho_s - \rho_w}\ \frac{\nu\ \hat{U}}{c\ g}\ [(\frac{c}{c_0})^{1/3} - 1]^{-3/2}\ \text{cotan}\ \alpha} \tag{20}$$

The time-dependent intrusiondepth H is given by eq.(17).

3.3. Results.
Figure 6 shows some results of the calculated variation (according eq.(14)) of the concentration during half a wave period, compared with the measurements of Horikawa et al (1982). In an oscillating water tunnel Horikawa carried out a series of laboratory experiments under sheet flow condition. The following deals with his experiment 1-1 with a period of 3.6 sec and a maximum orbital velocity of 1.27 m/sec.
Figure 7 gives the intrusion depth (point of zero velocity) of the sheet flow layer as function of time, also compared with the results of Horikawa et al. The depth H has to be taken, starting from a time-averaged bottom level, which is higher than the still bottom level. (The zero-level in the plots of Horikawa). The maximum intrusion depth is assumed to occur at the time of maximum velocity at level z=0 (phase angle $\theta = 60^0$). The theory would predict "still-water-concentration" for $\theta = 15^0$ (60^0 minus a phase shift of 45^0). This tendency also follows from Horikawa's data and from the numerical method treated below (fig 13b).

4. NUMERICAL COMPUTATIONS.

4.1. Grain-grain interactions in the numerical model
In the numerical model the motion of each layer of grains is considered separately; each layer exists of a rigid rectangular structure of spherical grains (Fig 1b). Grain- grain interaction between the successive layers occurs in two ways: on one hand viscous interaction forces, comparable with squeezing forces in lubrication problems and on the other hand direct contact with elastic response when the distance between the grains becomes less than .01 of the grain diameter. When the relative motion of adjacent layers results into compression or dilatation, a resistant force analogous to the Darcy law is assumed The viscous interaction forces are reproduced in the following way.
Let F_s be the Stokes force, exerted on a sphere, moving with velocity u in a fluid:

$$F_s = 6\ \pi\ \rho_w\ \nu\ u\ R \tag{21}$$

in which R is the radius of the sphere.
Many scientists investigated the increase of this force, when this sphere move to a wall, for instance Lorentz (1907).For the behaviour of the compression force in the immediate vicinity of the wall. Cox and Brenner (1967) find as asymptotic expansion:

$$F/F_s = \varepsilon^{-1} \; (1 - .2\varepsilon \ln \varepsilon + .9712\, \varepsilon) \tag{22}$$

$$\text{where: } \varepsilon = e_1/R \tag{23}$$

and e_1 is the distance between wall and sphere.
Truncating still earlier, one finds a lubrication limit, attributed to Taylor by Ambari et al (1984)

$$F/F_s = 1/\varepsilon \tag{24}$$

In the numerical model, in the contact points between the grains of two successive layers a contact force according to (24) has been assumed, where e_1 is taken as the distance between the spheres.
This force acts on the grains, resulting in a elastic compression, according to Timoshenko and Godier (1951) equal to:

$$\Delta s = A\, F^{2/3} \tag{25}$$

$$\text{in which: } A = \frac{9}{2}\left[\frac{(1 - \nu_c^2)^2}{E^2\, R}\right]^{1/3} \tag{26}$$

where ν_c is the contraction coefficient
Thus the distance between the centers of two grains becomes $2R - \Delta s$; from the two equations (22) and (25) for F the quantity Δs may be eliminated; F can be related to the distance between the centers of the grains of two successive layers.
In order to demonstrate the resulting way of collision, fig.$9^{a..d}$ shows the motion of the center of gravity y and of the grain surface x when a (smooth) sphere approaches a wall, starting with a certain velocity; this velocity increases in the various figures a..d. In fig. $9^{a..c}$ the sphere comes to rest at a certain distance from the wall, eventually after some elastic rebound. In fig 9^d the suction forces between sphere and wall exceed the cavitation limit of the fluid, which liberates the sphere from the wall: an elastic rebound occurs.

Also in the numerical model for the grain piling a tetrahedral piling is assumed.The effect of protuberances is taken into account, with direct contact with elastic response when the distance between the grains becomes less than .01 times the grain diameter. Fig 8 shows the way of motion of the grains. Each grain falls in the hole, shaped by 4 other grains on a lower level. In the equation of motion in horizontal direction sand and water are taken together; in vertical direction sand and water are treated separately, where inertia effects have been taken into account. With respect to friction, a drag coefficient similar to eq. (7) is assumed.
Apart from the friction, resulting from the horizontal components of the pressures in the contact points, viscous friction between the various layers is taken into account

The model of the sheetflow layer disposed here has been combined with the near- bottom velocity model, exposed by Bakker and van Kesteren (1984). In this implicit model, the shear stress τ_b at the top of the sheet flow layer has been determined from the local velocity gradient:

$$\tau_b = \rho_w \kappa^2 z^2 \, \frac{u_2 - u_1}{\Delta z} \left|\frac{u_2 - u_1}{\Delta z}\right| \tag{27}$$

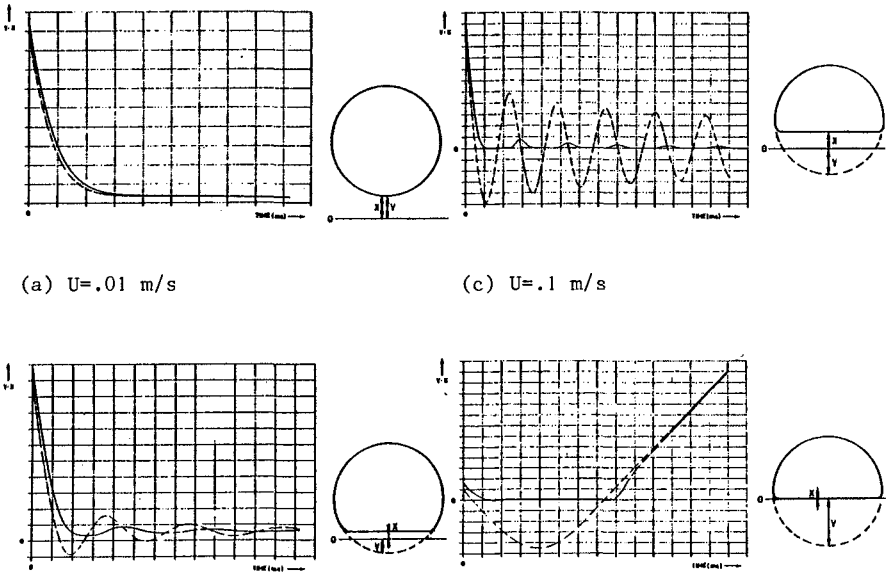

(a) U=.01 m/s

(c) U=.1 m/s

(b) U=.05 m/s

R=.1 mm, E=10 GPa, $\nu=10^{-6} m^2/s$

(d) U=1 m/s

—— x = distance sphere surface to wall

- - - - y = distance sphere centre to wall minus sphere radius

Fig.9 Visco-elastic collision of sphere with wall.

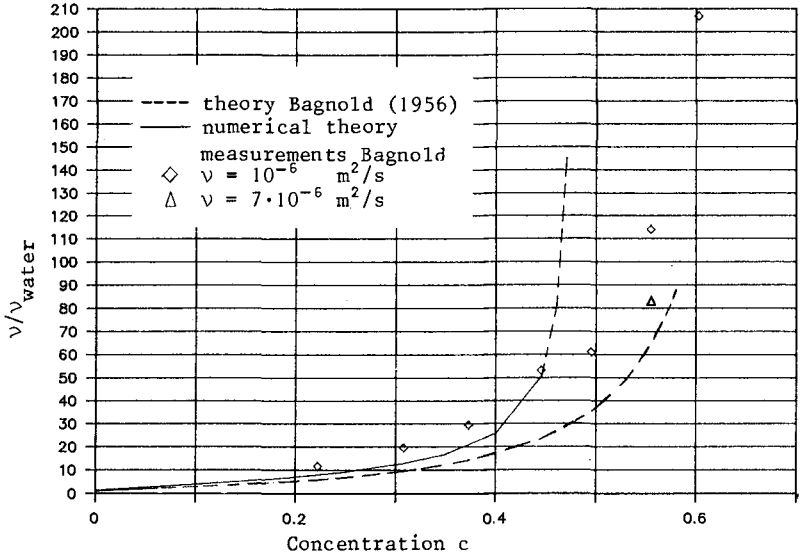

Fig.10 Increase of appearent viscosity as function of the concentration

where u_1 is the velocity of the upper sheet flow layer and u_2 of the first grid point in the (pure) water; the constant κ is the von Karman constant. The level "z=0" has been chosen at the still- sand level, starting from the intuitive feeling that the mixing length κz should be of the order of the vertical motion of the top of the sheetflow layer.

4.2. Results.

In this chapter the results of the numerical model are compared with experiments of Bagnold (1956) and Horikawa (1982)

Fig. 10 shows the results of a numerical simulation of plain shear, applied on grains with the same weight as the surrounding fluid. From this the increase of the concentration on pseudo- viscosity can be investigated. With the assumption of uniform shear between two parallel planes the motion becomes symmetrical, thus giving parallel motion of all the layers. Thus blocking is found when the grains in the layers can not slide between each other without transversal displacement. This occurs for a concentration higher than 48 %. Furthermore the increase in viscosity agrees rather well with Bagnold 's theory and measurements (fig 10).

However, where Bagnold experimentally finds a ratio between normal stress and shear stress equal to .75, the numerical model gives time-averaged normal stresses which are much lower. This is about as could be expected: for concentrations less than 48 % the grains move straight forward without hindering each other too much.

Fig 11 to 14 show the results of an experiment of Horikawa (1982), which has been numerically simulated.

Fig 11^a shows a comparison between measurements and numerical results concerning the velocity profile. Fig 11^b shows the velocities in the various sheetflow layers as function of time; totally 9 layers were mobilized. Layer 1 is the upper one. For the elasticity module a value of 10 MPa has been taken; however, similar computations with soft grains with an elasticity modulus of .1 MPa gave similar results. This indicates, that the effect of the viscous squeezing is much more of importance than the elasticity. Fig 13^a shows the concentration in the grain layers; the numerical model "chooses" its own concentration, depending on the interaction forces between the various layers. In the Horikawa experiment, this concentration is 74 % when the material is in rest (densiest packing) and about 60 % when the material is moving. The same appears from fig 13^b, giving the concentration profiles at various times.

Fig 12 gives the shear stress in the course of time for layer 1 and layer 9. Because in this case gravity takes care for vertical shifting of the layers (different from the Bagnold case), the pattern.is rather irregular. Therefore also the first harmonics are drawn; from this it shows, that the result of the analytical theory, a shear stress , constant per layer and increasing with the depth is too naive. The shear stress as found from the numerical model is not determined by the own weight of the grains, but by the shear stress on the surface. The result of the Bagnold theory of the constant ratio between shear stress and normal stress is checked also in fig 14, giving this ratio as it follows from the mathematical model. In the lower layers, which keep in rest, this ratio decreases gradually (starting from .75)

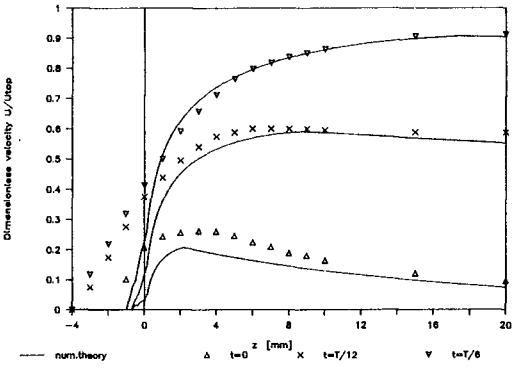

measurements from Horikawa (1982): exp.(1-1)

Fig.11a Velocity profiles at various times (num.comp.).

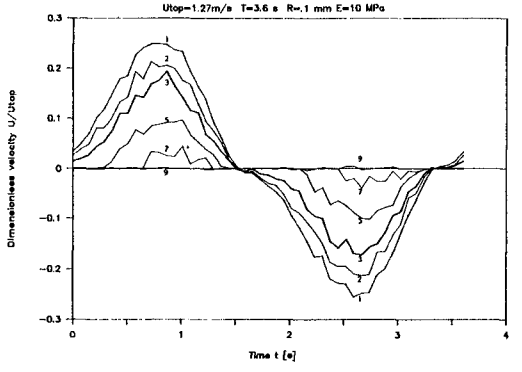

Fig.11b Velocity of the grain layers 1,2,3,5,7 and 9 (num.comp.).

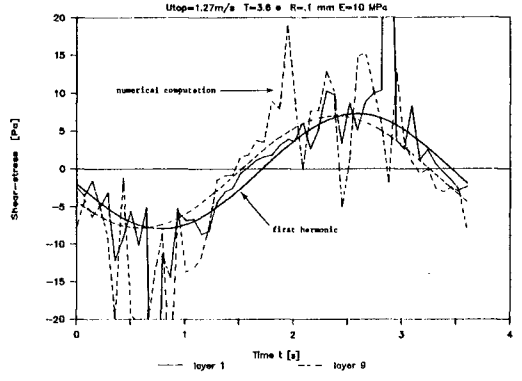

Fig.12 Shear stress in the grain layers 1 and 9 (num.comp.).

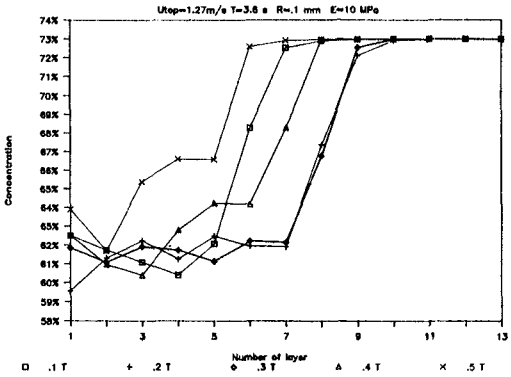

Fig.13a Concentration profiles at various times (num.comp.).

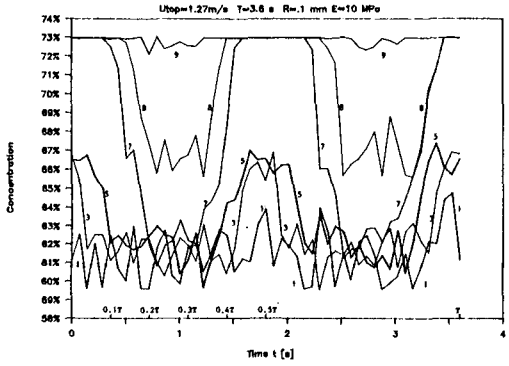

Fig.13b Concentration in the grain layers 1,3,5,7,8 and 9 (num.comp.).

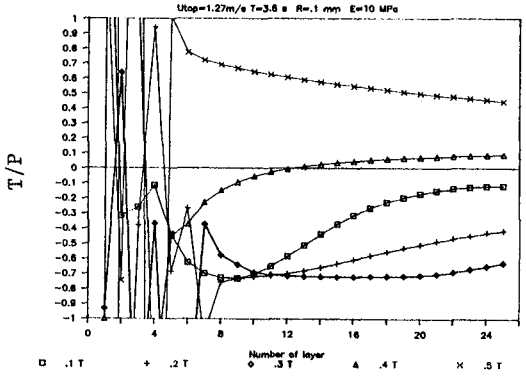

Fig.14 Ratio "shear stress / normal stress" at various times (num.comp).

because of the increasing own weight. In the higher layers, which are in motion, the ratio varies randomly between +10 and -10
It shows, that the numerical model does not tally quite with Bagnold's theory with respect to the dispersive stress.However, the physics of the Bagnold theory is not quite clear.
Indeed, one finds in the viscous region a "transverse pressure analogous to that which occurs in the static arching of grains in contact ", as stated by Bagnold (1954) ("a transverse dispersive tendency of a dense overtaking motor traffic along a one-way road").
However, in the numerical model grains moving from each other after a "collision" tear the layers from each other, by inertia of the grains, combined with viscous forces. This gives tension forces between the grains of the same order as the pressure forces. Where the pressure forces are more vigorous, the tension forces are more persistent, resulting in a very small value of the normal pressure. This appears from calculations with simplified models.
Furthermore dispersive forces are created by the convective terms in the equation of motion for the water in the pores between the grains. In the numerical model, these terms appear to be only a few percent of the shear stress. On one hand this follows from calculations in which the convective terms were left out, on the other hand by simplified calculations in which only this effect was taken into account.
From these calculations one finds a timeaveraged vertical pressure gradient of the order of magnitude of the energy of the vertical motion on the top of the shear flow layer.This vertical motion appears to be in the model only a few mm/sec.
Altogether the impression arises, that the motion on the top of the shear flow layer is too small; the motion is too smooth with as a result, that the shear stresses are too low and therefore the intrusion depth too small: in the numerical model the intrusion depth is 1.5 mm and in the Horikawa experiments 5 mm.
On the other hand Horikawa et al might have overestimated the transport somewhat, although this certainly will not explain the difference in order of magnitude.
Before the grains are able to move the grain structure first has to adopt a somewhat higher porosity. Therefore the highest point with zero amplitude, which determines the lower boundary of the velocity profile of the sheetflow-layer will be higher than the highest point of zero dilatation (cp. fig 11 and 12). This has not been taken into account by Horikawa et al (1982).

5. CONCLUSIONS.

Comparing analytical and numerical model with one of the experimental results of Horikawa et al (1982) leads to the following conclusions:

a. The analytical model reproduces concentration profiles and intrusion depth reasonably well (fig 6 and 7)). Assumptions about velocity profile and shear stress distribution however are too primitive (cp. fig 5 and fig 11 for analytical and numerical computations respectively).
b. Use of the Bagnold theory of constant shear stress ratio in the analytical model leads to better approximation of the intrusion depth than in the numerical model. The numerical model underestimates this depth.
However, the physics of the Bagnold theory is not quite clear.

Indeed, one finds in the viscous region a "transverse pressure analogous to that which occurs in the static arching of grains in contact ", as stated by Bagnold (1954). However, in the numerical model grains moving from each other after a "collision" tear the layers from each other, by inertia of the grains, combined with viscous forces. This gives tension forces between the grains of the same order as the pressure forces. Where the pressure forces are more vigorous, the tension forces are more persistent, resulting in a very small value of the normal pressure.
Furthermore dispersive forces are created by the convective terms in the equation of motion for the water in the pores between the grains. In the numerical model, these terms appear to be only a few percent of the shear stress.
In the numerical model the ratio between pressure and shear stress as found by Bagnold is only a continuous function of depth in the region with no significant motion (fig 14). In the sheetflow layers, the ratio varies at random between +10 and -10.
The increase of viscosity as found by Bagnold reproduces rather well in the numerical model (fig 10). However, simulating numerically the experimental set-up of Bagnold (grains with the same weight as the fluid) in the model a total blocking occurs at a concentration of 48 %, due to a schematization, which is too regular.

c. Of the two possibilities of the numerical model for transferring grain forces from one layer to another: (by "lubrication" or by direct elastic contact), the effect of lubrication appears to be the most important. This appears from comparitive calculations with various values of the elasticity of the grains, which did not have much effect on the intrusion depth of the sheetflow

d. The impression rises, - as well from the velocity distribution as from the intrusion depth - that the present numerical model is too smooth. In this model the transition between sheet flow layer and the uper layer is not yet well reproduced. One might expect here a transition layer with high turbulence, as occurs in density currents. This will give higher shear stress and higher vertical gradients of time- averaged vertical pressures, probably resulting in a higher intrusion depth of the sheetflow.

e. Before the grains are able to move the grain structure first has to adopt a somewhat higher porosity. Therefore the highest point with zero amplitude, which determines the lower boundary of the velocity profile of the sheetflow-layer will be higher than the highest point of zero dilatation (cp. fig 11 and 12). This has not been taken into account by Horikawa et al (1982). This might lead to overestimation of the transport.

f. A more extensive experimental verification of the theory under a broad range of circumstances is needed. For this goal a large pulsating water tunnel is constructed in the Delft Hydraulics Laboratory.

6. ACKNOWLEDGEMENT.

The authors are indebted to prof. K. Horikawa for sending additional information about his experiments. Mr. E. Haak carried out very useful computations. Financial support by the Royal Dutch Society for Sciences and by Rijkswaterstaat is gratefully acknowledged.

7. REFERENCES.

Ambari,A., B. Gauthiar-Manuel and E. Guyon,
Wail effects on a sphare, translating at constant valocity
J. Fluid Mech. 149, pp 235-253 (1984).
Bagnoid, R.A.,
Eperiments on a gravity-frae disparaion of larga soiid
apheres in a Newtonlan fluid under shear.
Proc. Royal Society, Voi. 225, A, p. 49 (1954).
Bagnold, R.A.,
The flow of cohesionlasa grains in fluids,
Proc, Royal Society, Voi. 249, A964, p. 235, Dacembar 18 (1956).
Bakker, W.T.,
Sand concentration in an osciliatory fiow,
Proc. 14th Conf. on Coastai Engng. Copenhagen (i974).
Bakker, W.T. and Van Kesteren, W.G.M.,
Near-bottom velocitiea in wavea with a current:
analyticai and numerical computations
Proc. 19th Conf. on Coastal Engng., Houston (i984).
Cox,R.G. and M.Branner,
The slow motion of a sphera through a viscous fluid towards a plana
surface - II Small gap, including inertial effects.
Chem. Engng. Sci. 22, i753 - i777 (1967).
Morikawa, K., Watanaba, A., and Katori, S.,
Sediment transport under sheet fiow condition.
Proc. 18th Conf. on Coastal Engng. Cape Town (i982).
Lorentz, H.A.,
Abhandl.theor. Physik, Leipzig i, 23 (1907).
Timoshenko, S.P. and Godier, J.N.,
Theory of elasticity,
Mc Graw Hiil, New York (i951).

8. NOTATION.

a		drag coefficient (eq.(7)).
A	$[m/N^{2/3}]$	stiffness parameter in elastic grain deformation (eq.(25).
b		horizontai distance / grain diametar betwaen grains in tetrahedralrectangular piiing.
c		concentration.
c_0		concentration at maximum density.
c_ℓ		limit concentration in the sheetflow (eq.(15)).
D	$[m]$	grain diameter.
e	$[m]$	spacing between spheres.
E	$[N/m^2]$	Youngs moduius of the grains.
F	$[N]$	grain interaction force.
F_s	$[N]$	Stokes force (eq.(21)).
g	$[m/a^2]$	acceleration of gravity.
h		vertical distance over grain diameter between centres of adjacent grainiayers.
h_0		value of h in the ciosest packing of grainiayars in tha sheetflow.
H	$[m]$	intrusion depth.
k	$[m/a]$	coefficient of permeability.
N		Bagnold-number (eq.(2)).
p	$[Pa]$	grain force due to vertical diapersive prassura gradient (eq.(5)).
p_0	$[Pa]$	mean of p (eq.(6)).
p_2	$[Pa]$	second harmonic of p (eq.(6)).
P	$[Pa]$	dispersive grain prassure.
R	$[m]$	grain radius.
Δs	$[m]$	elastic grain distorsion (eq.(25)).
T	$[Pa]$	effective grain ahear stress.
u	$[m/s]$	horizontal veiocity
U	$[m/s]$	horizontai vaiocity at top of tha sheetflow.
z	$[m]$	vertical coordinata (pos. upwards).
z_ℓ	$[m]$	vertical coordinate of grainlayer.
Z^g	$[m]$	verticai length scaie in tha sheatflow (aq.(12)).
α	$[deg]$	angle of intarnal friction.
ε		spacing between grains over grainradius (aq.(23)).
θ	$[deg]$	phase angle of osciiiating motion.
κ		Von Karman constant (eq.(27)).
λ		linear concentration (eq.(ic)).
ν	$[m^2/s]$	kinematic viscosity.
ρ_w	$[kg/m^3]$	specific density of water.
ρ_s	$[kg/m^3]$	specific density of sand.
τ_b	$[Pa]$	shear stress at the top of the sheetfiow.
ω	$[s^{-1}]$	anguiar frequency of the osciliating motion.
$\dot{x}$		time-derivative of x.
$\bar{x}$		mean value of x.
x_*		amplitude of x.
x		dimensionless value of x.
Δx		increment of x.